On penalty flux parameters in first order DG formulations

Jesse Chan, T. Warburton

Contents

1 Introduction

2 DG numerical fluxes

We consider a first order system of hyperbolic equations

$$\boldsymbol{A}_0 \frac{\partial \boldsymbol{U}}{\partial t} + \sum_{i=1}^{d} \frac{\partial \boldsymbol{F}_i(\boldsymbol{U})}{\partial \boldsymbol{x}_i} = 0,$$

which may alternatively be written as

$$\boldsymbol{A}_0 \frac{\partial \boldsymbol{U}}{\partial t} + \sum_{i=1}^{d} \frac{\partial \left(\boldsymbol{A}_i U\right)}{\partial \boldsymbol{x}_i}, \qquad \boldsymbol{A}_i = \frac{\partial \boldsymbol{F}_i(\boldsymbol{U})}{\partial \boldsymbol{U}}$$

where $\boldsymbol{A}_i$ are symmetric matrices. The semi-discrete DG formulation for such systems may be written as

$$\sum_{D^k \in \Omega_h} \left(\boldsymbol{A}_0 \frac{\partial \boldsymbol{U}}{\partial t}, \boldsymbol{V} \right)_{L^2(D^k)} = \sum_{D^k \in \Omega_h} \left((\boldsymbol{F}_i(\boldsymbol{U}), \boldsymbol{V}_{,i})_{L^2(D^k)} - \langle \boldsymbol{F}_n^*(\boldsymbol{U}) \boldsymbol{n}_i, \boldsymbol{V} \rangle_{\partial D^k} \right)$$

where $\boldsymbol{n}$ is the outward normal on a face f of D^k, and $\boldsymbol{F}_n^*$ is a numerical flux depending defined on shared faces between two elements.

Let f be a shared face between two elements $D^{k,+}$ and $D^{k,-}$, and let $\boldsymbol{F}^+, \boldsymbol{F}^-$ be evaluations of $\boldsymbol{F}(\boldsymbol{U})$ restricted to $D^{k,+}$ and $D^{k,-}$, respectively. The average and jump of a vector valued function over f are then defined as

$$\{\{\boldsymbol{F}\}\} = \frac{\boldsymbol{F}^+ + \boldsymbol{F}^-}{2}, \qquad [\![\boldsymbol{F}]\!] = \boldsymbol{F}^+ - \boldsymbol{F}^-.$$

Typical numerical fluxes are defined as the sum of the average of $\boldsymbol{F}^+$ and $\boldsymbol{F}^-$ and a penalization term

$$\boldsymbol{F}_n^* = \{\{\boldsymbol{F}(\boldsymbol{U})\}\} \cdot \boldsymbol{n} - \boldsymbol{G}\left([\![\boldsymbol{U}]\!]\right), \tag{1}$$

where $\boldsymbol{G}$ is some convex function.

The upwind numerical flux is a well-known flux of the form (1). For some normal vector $\boldsymbol{n}$, let $\boldsymbol{A}_n = \sum_{i=1}^d \boldsymbol{A}_i \boldsymbol{n}_i$. By add citation, $\boldsymbol{A}_n$ contains real eigenvalues, and admits an eigenvalue decomposition

$$\boldsymbol{A}_n = \boldsymbol{V}\boldsymbol{\Lambda}\boldsymbol{V}^{-1}, \qquad \boldsymbol{\Lambda} = \begin{pmatrix} \lambda_1 & & \\ & \ddots & \\ & & \lambda_d \end{pmatrix}.$$

For problems with continuous coefficients, the upwind numerical flux can be defined as

$$\boldsymbol{F}_n^* = \boldsymbol{A}_n^+ \boldsymbol{U}^- + \boldsymbol{A}_{\boldsymbol{n}}^- \boldsymbol{U}^+,$$

where the matrices $\boldsymbol{A}_{\boldsymbol{n}}^+, \boldsymbol{A}_{\boldsymbol{n}}^-$ are constructed from the positive and negative eigenvalues

$$\begin{aligned} \boldsymbol{A}_n^+ &= \frac{1}{2}\boldsymbol{V}\left(\boldsymbol{\Lambda} + |\boldsymbol{\Lambda}|\right)\boldsymbol{V}^{-1} \\ \boldsymbol{A}_n^- &= \frac{1}{2}\boldsymbol{V}\left(\boldsymbol{\Lambda} - |\boldsymbol{\Lambda}|\right)\boldsymbol{V}^{-1}, \end{aligned}$$

and $|\boldsymbol{\Lambda}|$ is the diagonal matrix whose entries consist of the absolute values of the eigenvalues $|\lambda_i|$. This can be rewritten as the sum of the central flux and a penalization

$$\boldsymbol{F}_n^* = \{\{\boldsymbol{A}_n \boldsymbol{U}\}\} - \tau \boldsymbol{V}\left|\boldsymbol{\Lambda}\right|\boldsymbol{V}^{-1}[\![\boldsymbol{U}]\!].$$

For problems with discontinuous coefficients, this may be generalized by solving a Riemann problem to yield

$$\boldsymbol{F}_n^* = \{\{\boldsymbol{A}_n \boldsymbol{U}\}\} - \tau[\![\boldsymbol{V}\left|\boldsymbol{\Lambda}\right|\boldsymbol{V}^{-1}\boldsymbol{U}]\!].$$

An alternative to upwind fluxes are penalty fluxes, which penalize appropriately defined jumps of the solution. One such penalty flux is

$$\boldsymbol{F}_n^* = \{\{\boldsymbol{A}_n \boldsymbol{U}\}\} - \boldsymbol{A}_n^T \boldsymbol{W}[\![\boldsymbol{A}_n \boldsymbol{U}]\!].$$

where $\boldsymbol{W}$ is a diagonal weighting matrix with positive entries. We take $\boldsymbol{W} = \tau \boldsymbol{I}$ in the following sections; however, the entries can be made to vary. For example, taking $\boldsymbol{W} = |\boldsymbol{\Lambda}|^{-1}$ recovers the upwind fluxes prove this.

2.1 Examples: acoustic wave equation

Consider the isotropic acoustic wave equation in pressure-velocity form

$$\begin{aligned} \frac{\partial p}{\partial t} &= \nabla \cdot \boldsymbol{u} \\ \frac{\partial \boldsymbol{u}}{\partial t} &= \nabla p. \end{aligned}$$

Let $\boldsymbol{U}$ denote the group variable $\boldsymbol{U} = (p, u, v)$, where u and v are the x and y components of velocity. Then, in two dimensions, the isotropic wave equation is given as

$$\frac{\partial \boldsymbol{U}}{\partial t} + \frac{\partial \boldsymbol{A}_x \boldsymbol{U}}{\partial x} + \frac{\partial \boldsymbol{A}_y \boldsymbol{U}}{\partial y} = 0, \qquad \boldsymbol{A}_x = \begin{pmatrix} 0 & 1 & 0 \\ 1 & 0 & 0 \\ 0 & 0 & 0 \end{pmatrix}, \qquad \boldsymbol{A}_y = \begin{pmatrix} 0 & 0 & 1 \\ 0 & 0 & 0 \\ 1 & 0 & 0 \end{pmatrix}.$$

The normal flux matrix $\boldsymbol{A}_n$ is then

$$\boldsymbol{A}_n = \begin{pmatrix} 0 & \boldsymbol{n}_x & \boldsymbol{n}_y \\ \boldsymbol{n}_x & 0 & 0 \\ \boldsymbol{n}_y & 0 & 0 \end{pmatrix}$$

implying that the penalty fluxes (with $\boldsymbol{W} = \tau \boldsymbol{I}$) are

$$\{\{\boldsymbol{A}_n \boldsymbol{U}\}\} - \tau \boldsymbol{A}_n^T [\![\boldsymbol{A}_n \boldsymbol{U}]\!] = \begin{pmatrix} \{\{\boldsymbol{u}_n\}\} \\ \{\{p\}\}\, \boldsymbol{n}_x \\ \{\{p\}\}\, \boldsymbol{n}_y \end{pmatrix} - \tau \begin{pmatrix} [\![p]\!] \\ [\![\boldsymbol{u}_{\boldsymbol{n}}]\!] \boldsymbol{n}_x \\ [\![\boldsymbol{u}_{\boldsymbol{n}}]\!] \boldsymbol{n}_y \end{pmatrix}$$

For $\tau = 1$, these fluxes coincide with the upwind fluxes for isotropic media. We note that the penalty flux affects only the normal component of the velocity; this is in contrast to Lax-Friedrichs-type fluxes, which penalize component-wise discontinuities in the velocity.

Skew-symmetric discretization for constant coefficient problems [1]. For wave propagation, can wrap variable coefficients into A_0 [2, 3].

3 Dependence of spectra on the penalty parameter

Define spaces and show that $\boldsymbol{S}$ is symmetric definite based on DG discretization.

We adapt the proof presented in [4] to show that the spectra of $\boldsymbol{K}$ splits into two sets as $\tau \to \infty$, the first of which approaches the eigenvalues of $\boldsymbol{A}$, and the second of which moves left of the imaginary axis at a rate of $O(\tau)$.

We begin by splitting the DG approximation space into a conforming part V^C and a non-conforming part V^{NC}. Let V be the DG approximation space

$$V = \left\{ u \in L^2(\Omega_h) : u|_{D^k} \in P^N(D^k) \right\}.$$

The conforming space V^C is then defined as

$$V^C = \{ u(\boldsymbol{x}) \in V : \} \tag{2}$$

We can similarly define the non-conforming approximation space V^{NC} as the orthogonal complement of V^C, such that the full approximation space V is

$$V = V^C \oplus V^{NC}.$$

This induces a block decomposition

$$\boldsymbol{K} = \begin{pmatrix} \boldsymbol{A} & \boldsymbol{B} \\ -\boldsymbol{B}^T & \boldsymbol{C} + \tau \boldsymbol{S} \end{pmatrix}.$$

We first consider the spectra of $\boldsymbol{C} + \tau \boldsymbol{S}$. By the construction of the DG formulation $\boldsymbol{C}$ is skew-symmetric, while $\boldsymbol{S}$ is symmetric and negative-definite. Let $\lambda, \boldsymbol{u}$ be an eigenpair of $\boldsymbol{C} + \tau \boldsymbol{S}$ corresponding to the largest N^D eigenvalues. Let $\lambda = \alpha + i\beta$ and $\boldsymbol{u} = \boldsymbol{v} + i\boldsymbol{w}$, where α, β and $\boldsymbol{v}, \boldsymbol{w}$ are the real and imaginary parts of λ and $\boldsymbol{u}$, respectively. Then, expanding and grouping terms in

$$(\boldsymbol{C} + \tau \boldsymbol{S})(\boldsymbol{v} + i\boldsymbol{w}) = (\alpha + i\beta)(\boldsymbol{v} + i\boldsymbol{w})$$

we have that

$$(\boldsymbol{C} + \tau \boldsymbol{S})\boldsymbol{v} = \alpha \boldsymbol{v} - \beta \boldsymbol{w}$$
$$(\boldsymbol{C} + \tau \boldsymbol{S})\boldsymbol{w} = \beta \boldsymbol{v} + \alpha \boldsymbol{w}.$$

Assuming that $\boldsymbol{u}^*\boldsymbol{u} = \|\boldsymbol{v}\|^2 + \|\boldsymbol{w}\|^2 = 1$, multiplying both sides by $\boldsymbol{v}^T, \boldsymbol{w}^T$ and straightforward manipulations using the skew-symmetry of $\boldsymbol{C}$ and symmetry of $\boldsymbol{S}$ yields

$$\boldsymbol{v}^T\boldsymbol{C}\boldsymbol{w} - \boldsymbol{w}^T\boldsymbol{C}\boldsymbol{w} = \beta$$
$$\tau\left(\boldsymbol{v}^T\boldsymbol{S}\boldsymbol{v} + \boldsymbol{w}^T\boldsymbol{S}\boldsymbol{w}\right) = \alpha.$$

Since $\boldsymbol{v}^T\boldsymbol{C}\boldsymbol{w} - \boldsymbol{w}^T\boldsymbol{C}\boldsymbol{w} = 2\boldsymbol{w}^T\boldsymbol{C}\boldsymbol{v} = \beta$ is independent of τ and $\boldsymbol{v}, \boldsymbol{w}$ are normalized, β remains bounded as $\tau \to \infty$. Similarly, since $\boldsymbol{S}$ is symmetric, negative-definite, and independent of τ, the quantity

$$\left|\boldsymbol{v}^T\boldsymbol{S}\boldsymbol{v} + \boldsymbol{w}^T\boldsymbol{S}\boldsymbol{w}\right| = \left|\frac{\alpha}{\tau}\right|$$

is bounded independently of τ, and we conclude that $|\alpha| = O(\tau)$. Thus, as τ increases, the eigenvalues of $\boldsymbol{C} + \tau\boldsymbol{S}$ are shifted further and further left of the imaginary axis.

We may now show how the spectra of $\boldsymbol{K}$ behaves as $\tau \to \infty$. Following [4], let $\boldsymbol{U}$ and $\boldsymbol{Q}$ be unitary matrices whose columns contain the eigenvectors of $\boldsymbol{A}$ and $\boldsymbol{C} + \tau\boldsymbol{S}$, respectively. Then, applying a block diagonal similarity transform yields

$$\begin{pmatrix} \boldsymbol{U}^* & \\ & \boldsymbol{Q}^* \end{pmatrix} \begin{pmatrix} \boldsymbol{A} & \boldsymbol{B} \\ -\boldsymbol{B}^T & \boldsymbol{C} + \tau\boldsymbol{S} \end{pmatrix} \begin{pmatrix} \boldsymbol{U} & \\ & \boldsymbol{Q} \end{pmatrix} = \begin{pmatrix} \boldsymbol{\Lambda}_C & \boldsymbol{U}^T\boldsymbol{B}\boldsymbol{Q} \\ -\boldsymbol{Q}^T\boldsymbol{B}^T\boldsymbol{U} & \boldsymbol{\Lambda}_D \end{pmatrix},$$

where $\boldsymbol{\Lambda}_C, \boldsymbol{\Lambda}_D$ are diagonal matrices whose entries consist of eigenvalues of $\boldsymbol{A}, \boldsymbol{C} + \tau\boldsymbol{S}$, respectively. Since $\boldsymbol{B}$ is independent of τ, $\left\|\boldsymbol{U}^T\boldsymbol{B}\boldsymbol{Q}\right\|$ can be bounded independently of τ, assuming that $\boldsymbol{U}$ and $\boldsymbol{Q}$ are normalized. Gerschgorin's theorem applied to $\boldsymbol{\Lambda}_C, \boldsymbol{\Lambda}_D$ then implies that the eigenvalues of $\boldsymbol{K}$ are contained in two sets of discs with radii independent of τ. The first set of discs are centered around λ_i^C for $i = 1, \ldots, N^C$, while the second set of discs are centered around λ_i^D for $i = 1, \ldots, N^D$, where $\mathrm{Re}(\lambda_i^D) = O(\tau)$.

Consider now the N^C eigenvalues with the smallest magnitude. By the Gerschgorin argument, these must remain bounded as $\tau \to \infty$. Let $\boldsymbol{W} = (\boldsymbol{W}_C, \boldsymbol{W}_D)$ and $\boldsymbol{\Lambda}_C$ be the matrix of eigenvectors and eigenvalues corresponding to these N^C smallest eigenvalues, such that

$$\begin{pmatrix} \boldsymbol{A} & \boldsymbol{B} \\ -\boldsymbol{B}^T & \boldsymbol{C} + \tau\boldsymbol{S} \end{pmatrix} \begin{pmatrix} \boldsymbol{W}_C \\ \boldsymbol{W}_D \end{pmatrix} = \begin{pmatrix} \boldsymbol{A}\boldsymbol{W}_C + \boldsymbol{B}\boldsymbol{W}_D \\ -\boldsymbol{B}^T\boldsymbol{W}_C + \boldsymbol{C}\boldsymbol{W}_D + \tau\boldsymbol{S}\boldsymbol{W}_D \end{pmatrix} = \boldsymbol{\Lambda}_C \begin{pmatrix} \boldsymbol{W}_C \\ \boldsymbol{W}_D \end{pmatrix}$$

This implies

$$\tau\left\|\boldsymbol{S}\boldsymbol{W}_D\right\| = \left\|\boldsymbol{\Lambda}_C\boldsymbol{W}_D + \boldsymbol{B}^T\boldsymbol{W}_C - \boldsymbol{C}\boldsymbol{W}_D\right\|.$$

Since Λ_C remains bounded as $\tau \to \infty$, the right hand side is bounded independently of τ under normalization of $\boldsymbol{W}_C, \boldsymbol{W}_D$, implying that the non-conforming component $\boldsymbol{W}^D$ satisfies

$$C\left\|\boldsymbol{W}_D\right\| \leq \left\|\boldsymbol{S}\boldsymbol{W}_D\right\| = O(1/\tau).$$

As a consequence, $\boldsymbol{W}_D \to 0$ as $\tau \to \infty$, and the smallest N^C eigenvalues of $\boldsymbol{K}$ converge to the purely imaginary eigenvalues of $\boldsymbol{A}$ at a rate of $O(1/\tau)$. These correspond to a discretization using the conforming approximation space (2).

4 Numerical experiments

The above analysis illustrates the behavior of the spectra of the DG discretization for the asymptotic cases when $\tau = 0$ or $\tau \to \infty$. However, it is less clear how the spectra of $\boldsymbol{K}$ behaves for $\tau = O(1)$. We rely instead on numerical experiments in one and two space dimensions to illustrate behaviors for the advection and acoustic wave equations.

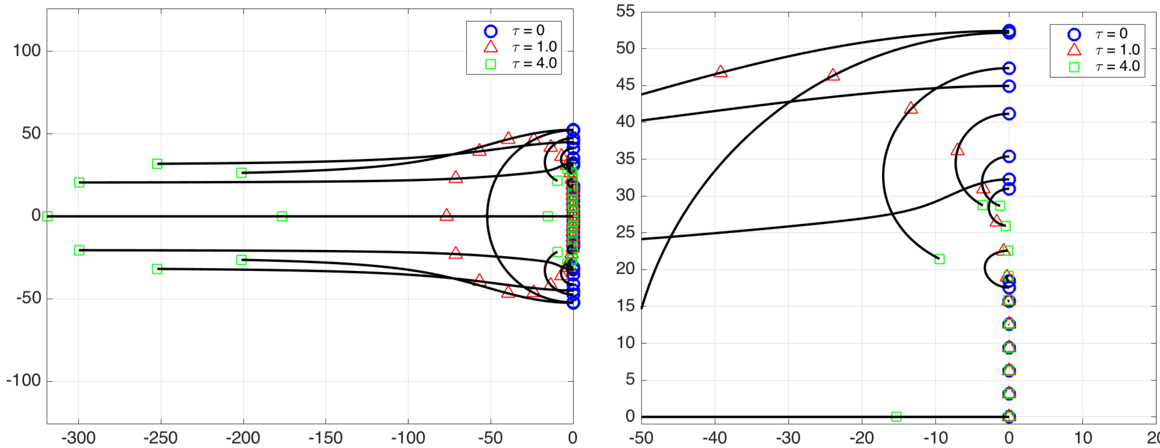

(a) Paths of eigenvalues as τ increases

(b) Zoom of eigenvalues near imaginary axis

Figure 1: Eigenvalue paths for DG advection with $\tau \in [0, 4]$ on a mesh of 8 elements of degree $N = 3$. Eigenvalues are overlaid on these paths for $\tau = 0$, $\tau = 1$, and $\tau = 4$. The zoomed in view near the imaginary axis shows the return of spurious modes to the imaginary axis for τ sufficiently large.

4.1 1D experiments

We consider first the scalar advection equation in 1D with periodic boundary conditions. For $\tau = 0$, the eigenvalues of the DG discretization matrix are purely imaginary. Figure 1 shows the paths taken by these eigenvalues as τ increases from zero to $\tau = 4$. As predicted, a subset of eigenvalues diverges towards the left half plane, which we refer to as *divergent*. The corresponding eigenmodes are shown in Figure 2, with inter-element jumps of these eigenfunctions increasing as τ increases.

However, for sufficiently large τ, a subset of eigenvalues return to the imaginary axis. Figure 3 illustrates that, as τ increases, the magnitude of the inter-element jumps present in these modes decreases, and the mode approaches a continuous function. These eigenvalues which return to the imaginary axis correspond to a second set of *spurious* modes, consisting of higher frequency components with sharp peaks, which have previously been observed in high order C^0 finite element methods [5, 6].

We repeat the above experiment for the acoustic wave equation in 1D with reflection boundary conditions on $[-1, 1]$, and compare against the exact eigenvalues $\lambda_i = i\frac{\pi}{2}$ for $i = 1, 2, \ldots$. The behavior of the eigenvalues as τ increases (Figure 6) is similar to the behavior observed for the scalar advection equation. An examination of the eigenmodes corresponding to divergent and spurious eigenvalues as $\tau \to \infty$ shows that these modes behave similarly to the spurious modes observed for the scalar advection equation, with individual pressure and velocity components converging to continuous functions.

4.2 2D experiments

In two space dimensions, taking $\tau \to \infty$ again results in spurious modes which return to the imaginary axis. The corresponding eigenvalues converge to conforming functions. For the acoustic wave equation, p is continuous across faces, edges, and vertices, implying that $p \in H^1(\Omega_h)$, while only the normal component of $\boldsymbol{u}$ is continuous across faces, implying that $\boldsymbol{u} \in H(\text{div}; \Omega_h)$.

Uniform triangular mesh resulting from bisecting each element of a 2×2 uniform quadrilateral mesh.

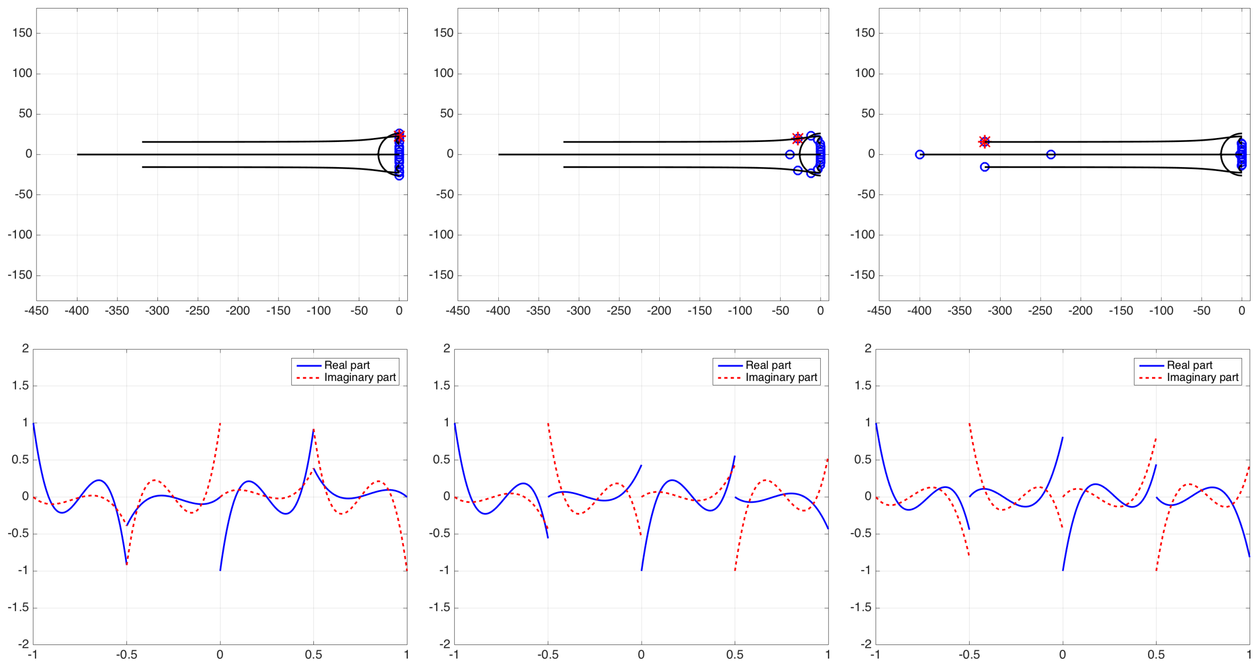

Figure 2: Behavior of divergent eigenvalues for advection as τ increases. The order of approximation is $N = 3$ on a mesh of 4 elements.

5 Conclusions

References

[1] David A Kopriva and Gregor J Gassner. An energy stable discontinuous Galerkin spectral element discretization for variable coefficient advection problems. *SIAM Journal on Scientific Computing*, 36(4):A2076–A2099, 2014.

[2] Jesse Chan, Russell J Hewett, and T Warburton. Weight-adjusted discontinuous Galerkin methods: wave propagation in heterogeneous media. *arXiv preprint arXiv:1608.01944*, 2016.

[3] Jesse Chan, Russell J Hewett, and T Warburton. Weight-adjusted discontinuous Galerkin methods: curvilinear meshes. *arXiv preprint arXiv:1608.03836*, 2016.

[4] T. Warburton and Mark Embree. The role of the penalty in the local discontinuous Galerkin method for Maxwell's eigenvalue problem. *Computer Methods in Applied Mechanics and Engineering*, 195(25-28):3205 – 3223, 2006.

[5] Mark Ainsworth. Dispersive behaviour of high order finite element schemes for the one-way wave equation. *Journal of Computational Physics*, 259:1–10, 2014.

[6] Thomas JR Hughes, John A Evans, and Alessandro Reali. Finite element and NURBS approximations of eigenvalue, boundary-value, and initial-value problems. *Computer Methods in Applied Mechanics and Engineering*, 272:290–320, 2014.

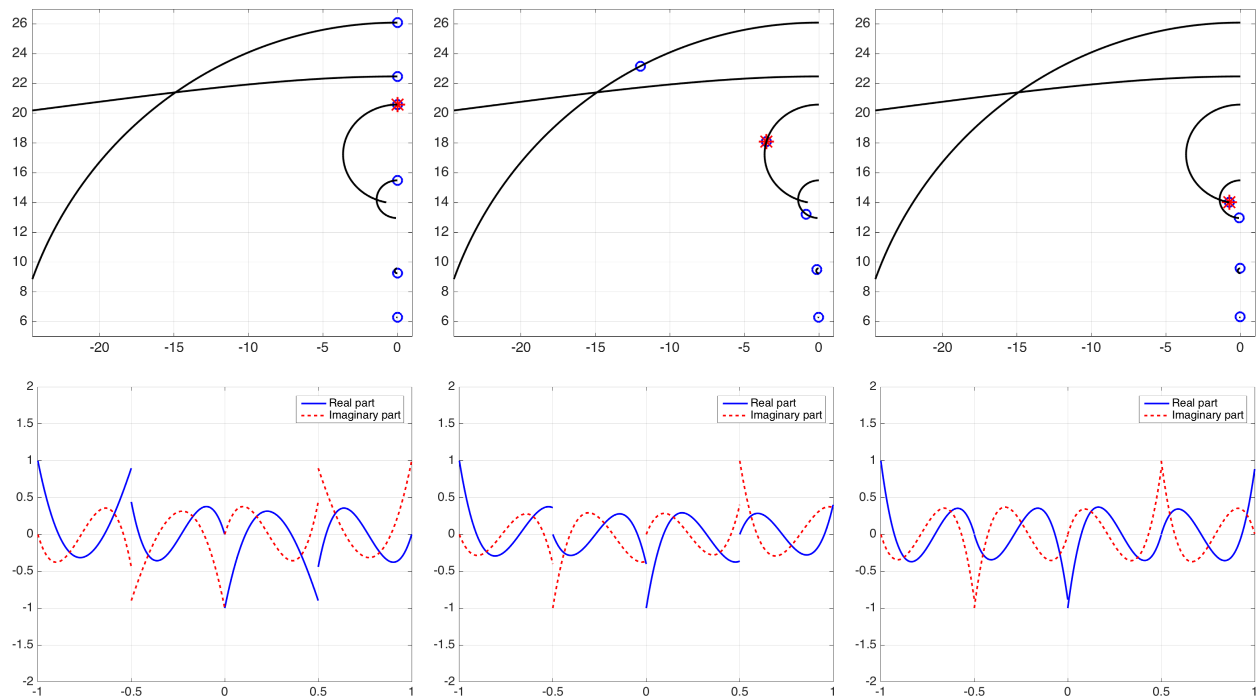

(d) $\tau = 0$ (e) $\tau = 1$ (f) $\tau = 10$

Figure 3: Return behavior of DG advection eigenvalues for sufficiently large τ. For $\tau = 1$ certain eigenvalues have negative real part, and the corresponding eigenmodes are damped. For $\tau \gg 1$, certain eigenvalues return to the imaginary axis as spurious modes in conforming discretizations.

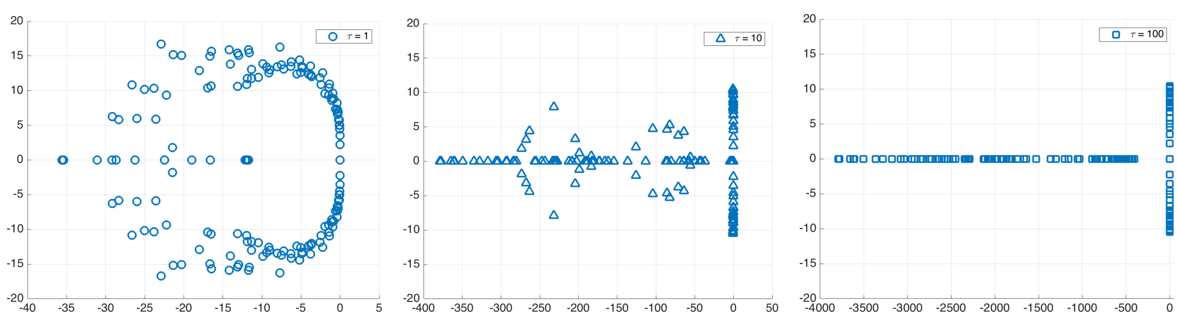

(a) $\tau = 1$ (b) $\tau = 10$ (c) $\tau = 100$

Figure 4: Behavior of eigenvalues for the acoustic wave equation in two dimensions. Note the changing scale of the real axis.

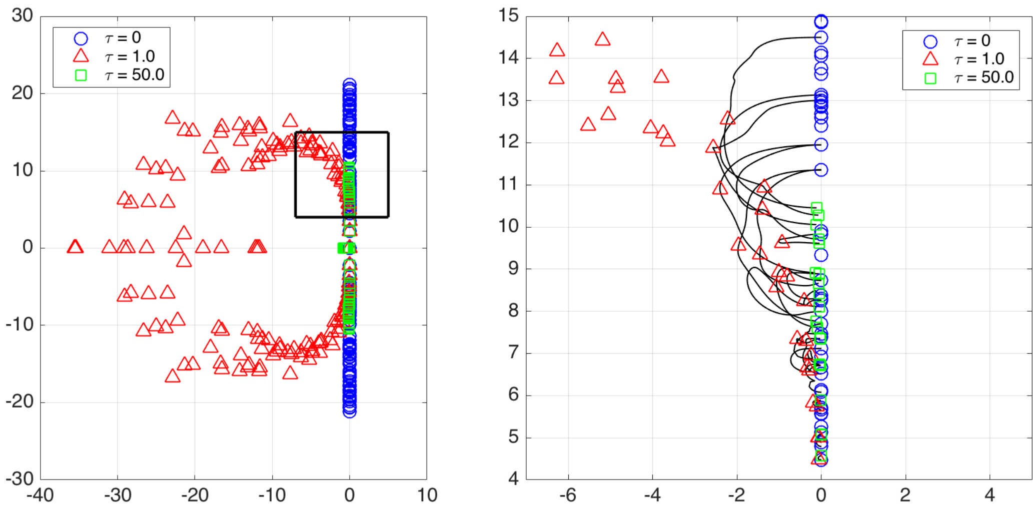

(a) $\tau = 0, 1, 50$, zoomed in view (b) $\tau = 0, 1, 50$, returning eigenvalue paths

Figure 5: Behavior of eigenvalues for the acoustic wave equation in two dimensions. Divergent eigenvalues in the far left half plane are not shown.

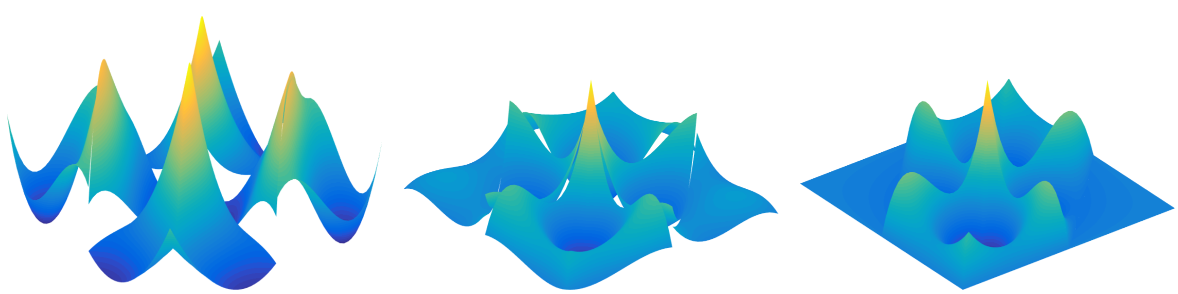

(a) $\tau = .1$, $\lambda = -0.2379 + 8.7528i$ (b) $\tau = 1$, $\lambda = -1.0145 + 8.9270i$ (c) $\tau = 50$, $\lambda = -0.0437 + 7.6167i$

Figure 6: Behavior of spurious returning modes for the acoustic wave equation in two dimensions.